Theor Chem Acc (2011) 129:793–801
DOI 10.1007/s00214-011-0937-5

REGULAR ARTICLE

Electronic spectra of the linear cationic chains $NC_{2n}N^+$ (n = 1–7): an ab initio study

Yuan Zhao · Jia Guo · Jinglai Zhang

Received: 15 February 2011 / Accepted: 4 April 2011 / Published online: 19 April 2011

Abstract The ground-state equilibrium geometries of the linear carbon chain cations $NC_{2n}N^+$ ($n = 1$–7) have been investigated with B3LYP, CAM-B3LYP, and RCCSD(T) calculations. The ground state ($X^2\Pi_{g/u}$) and excited state ($1^2\Pi_{u/g}$) have been optimized by using the complete active space self-consistent field method. The present study reveals that these linear cations generally have the characteristic of bond length alternation in both electronic states. The vertical excited energies for the dipole-allowed $(1, 2, 3)^2\Pi_{u/g} \leftarrow X^2\Pi_{g/u}$ transitions as well as the dipole-forbidden $1^2\Phi_{u/g} \leftarrow X^2\Pi_{g/u}$ transitions have been computed with the complete active space second-order perturbation theory. The calculated transition energies of $1^2\Pi_{u/g} \leftarrow X^2\Pi_{g/u}$ for $NC_{2n}N^+$ ($n = 1$–6) in the gas phase are 2.26, 2.09, 1.91, 1.72, 1.56, and 1.39 eV, respectively, which mutually agree well with the available experimental values of 2.11, 2.07, 1.88, 1.67, 1.49, and 1.34 eV. Moreover, the corresponding absorption wavelengths are predicted to have the significant nonlinear size dependence, which is different from the bands origin in $NC_{2n}N$ ($n = 1$–7).

Keywords $NC_{2n}N^+$ · Electronic spectra · Excited state · Ab initio study

Y. Zhao · J. Guo · J. Zhang (✉)
Institute of Environmental and Analytical Sciences,
College of Chemistry and Chemical Engineering,
Henan University, Kaifeng, Henan 475004,
People's Republic of China
e-mail: zhangjinglai@henu.edu.cn

1 Introduction

Nowadays, many astrophysicists are very interested in molecules and ions containing the CN group, which have been detected in interstellar clouds and atmospheres of carbon stars [1]. Moreover, the presence of neutral cyanopolyacetylenes in the interstellar medium is well established [2–4]. In addition, cyanopolyacetylenes and their cations are unstable molecules under usual terrestrial conditions that can react with a wide variety of atoms, thus, they have been the subject of several studies of reaction mechanisms that may be relevant to their production in astronomical environments [5]. Because of the important position of these species both in astrophysics and terrestrial processes, there has been a growing interest in experimental and theoretical studies on their structural and spectral properties [6–13]. In the last several decades, the cyanopolyacetylene cations $NC_{2n}N^+$ ($n = 1$–6) attracted considerable attention, and a large number of experimental and theoretical studies were performed on the species [10–13].

To our best knowledge, some collaborative studies have been taken on the properties of $NC_{2n}N^+$ ($n = 1$–6). Maier and co-workers observed the absorption spectra of $NC_{2n}N^+$ ($n = 1$–6) in 5 K neon matrices [10–12]. The bands origin for the $1^2\Pi_{u/g} \leftarrow X^2\Pi_{g/u}$ transition locates at 588, 598, 659, 741, 831, and 923 nm, respectively. Moreover, they obtained the absorption spectra of NC_2N^+, NC_4N^+, and NC_6N^+ in the gas phase, and the bands origin are 578, 596, and 656 nm, respectively [10]. They also measured the higher excited electronic transitions of NC_2N^+, NC_4N^+, and NC_6N^+ and found several new absorption bands.

Theoretically, Lee et al. [13] predicted the equilibrium geometries of ground state for $NC_{2n}N^+$ ($n = 2$–6) at UHF/4-31G level of theory. Moreover, they calculated the vertical transition energies for the $1^2\Pi_{u/g} \leftarrow X^2\Pi_{g/u}$ transition by the complete active space self-consistent field method (CASSCF) and the complete active space second-order perturbation theory method (CASPT2) with DZVP basis set [14–16]. However, they pointed out that it was a preliminary study, and the results were not good for some species. In addition, they did not find the size dependence of vertical excitation energies for $NC_{2n}N^+$. Cao et al. [17] also calculated the vertical transition energies of NC_4N^+ by using a multireference configuration interaction method (MRD-CI), and the values are 2.14 and 3.32 eV for the (1, 2)$^2\Pi_{u/g} \leftarrow X^2\Pi_{g/u}$ transition, respectively, while they just computed the cluster NC_4N^+, thus, the $NC_{2n}N^+$ system need more theoretical investigations.

Consequently, in order to interpret the experimental bands and enrich the chemical properties for these species systematically, the trustworthy theoretical calculations on the excited state properties of these linear cationic chains are highly required. In our previous calculations, the CASPT2 [18] theory has been used for $C_{2n+1}Cl^+$ ($n = 0$–4) [19], $HC_{2n}H^+$ ($n = 2$–8) [20], and $HC_{2n+1}H^+$ ($n = 2$–7) [21] clusters, and we got very excellent results. Therefore, in this paper, we have performed an extensive investigation on the vertical excitation energies of dipole-allowed (1, …, 3)$^2\Pi_{u/g} \leftarrow X^2\Pi_{g/u}$ transitions as well as the dipole-forbidden $1^2\Phi_{u/g} \leftarrow X^2\Pi_{g/u}$ transitions for the cations $NC_{2n}N^+$ ($n = 1$–7) at the CASPT2 level of theory. Moreover, we also discussed their structural characteristic, stabilities, and size dependences of the excited state properties. We hope that our calculations can provide reliable theory basis for the further experiment.

2 Computation details

The equilibrium geometries of linear carbon clusters $NC_{2n}N^+$ in their ground states have been optimized by RCCSD(T) method [22–24] with cc-pVTZ basis set [25–29] for $n = 1$–5, as well as 6-31G* basis set [30–40] for $n = 1$–7. The B3LYP [41–43] and CAM-B3LYP [44] density functionals with cc-pVTZ basis set optimized results are presented for a direct comparison. In addition, the geometries of the first excited state $1^2\Pi_{u/g}$ and ground state $X^2\Pi_{g/u}$ of $NC_{2n}N^+$ ($n = 1$–7) have been explored by the CASSCF method [45, 46] with 6-31G* basis set. Rotational constants have been calculated under the optimized geometries above, and the stability of optimized structures has been evaluated through the vibrational calculations.

The relative energies of the ground state and the excited electronic states of $NC_{2n}N^+$ ($n = 1$–7) have been computed by the complete active space second-order perturbation theory (CASPT2) method with the cc-pVTZ basis set [25–28, 47] at the RCCSD(T)/6-31G(d) and RCCSD(T)/cc-pVTZ equilibrium geometries. In the CASPT2 calculation, the CASSCF active space is generally composed of the low-energy π valence orbitals. In order to consider the electron correlation effect, the number of the active orbitals and electrons has been individually selected for each species, all of which are listed in Table 1. The first set of eight numbers mean the numbers of inactive (doubly occupied in each configuration) orbitals with symmetry labels A_g, B_{3u}, B_{2u}, B_{1g}, B_{1u}, B_{2g}, B_{3g}, and A_u, respectively, while the last eight numbers are the similar symmetry distribution number for the active orbitals.

Table 1 The CASSCF active spaces of $NC_{2n}N^+$ ($n = 1$–7) at the CASPT2 calculations

Species	CASSCF active space	Electrons
NC_2N^+	(5, 0, 0, 0, 4, 0, 0, 0/0, 2, 2, 0, 0, 2, 2, 0)	7
NC_4N^+	(7, 0, 0, 0, 6, 0, 0, 0/0, 3, 3, 0, 0, 2, 2, 0)	11
NC_6N^+	(9, 0, 0, 0, 8, 0, 0, 0/0, 3, 3, 0, 0, 2, 2, 0)	15
NC_8N^+	(11, 0, 0, 0, 10, 0, 0, 0/0, 3, 3, 0, 0, 3, 3, 0)	19
$NC_{10}N^+$	(13, 0, 0, 0, 12, 0, 0, 0/0, 4, 4, 0, 0, 3, 3, 0)	23
$NC_{12}N^+$	(15, 0, 0, 0, 14, 0, 0, 0/0, 4, 4, 0, 0, 4, 4, 0)	27
$NC_{14}N^+$	(17, 2, 2, 0, 16, 1, 1, 0/0, 3, 3, 0, 0, 3, 3, 0)	19

The oscillator strengths (f) are calculated with the following formula:

$$f = (2/3)\,\Delta E \mid \mathrm{TM} \mid^2 \qquad (1)$$

where ΔE denotes the transition energy between the ground state and the excited state in atomic unit, and TM is the transition moment in atomic unit [48].

All electronic structure calculations in the present work have been performed by the Gaussian 09 [49] and MOLPRO 2006 [50] program packages.

3 Results and discussion

3.1 Geometries and stabilities

3.1.1 The ground state geometries

The B3LYP, CAM-B3LYP, and RCCSD(T) optimized bond lengths of carbon clusters $NC_{2n}N^+$ ($n = 1$–7) in their ground states are displayed in Fig. 1. Compared to the RCCSD(T) results, both the B3LYP and CAM-B3LYP predict similar bond lengths of the equilibrium geometries. Moreover, Fig. 1 indicates that there is a character of bond length alternation (BLA) in $NC_{2n}N^+$ ($n = 1$–7), which is consistent with the previous studies on $C_{2n+1}Cl^+$ ($n = 0$–4) [19], $HC_{2n}H^+$ ($n = 2$–8) [20], $HC_{2n+1}H^+$ ($n = 2$–7) [21], and polyyne oligomers [51]. The character of BLA by CAM-B3LYP is significantly notable than those

Fig. 1 The optimized bond lengths (in Å) of $NC_{2n}N^+$ ($n = 1$–7) cations by B3LYP, CAM-B3LYP, and RCCSD(T) method

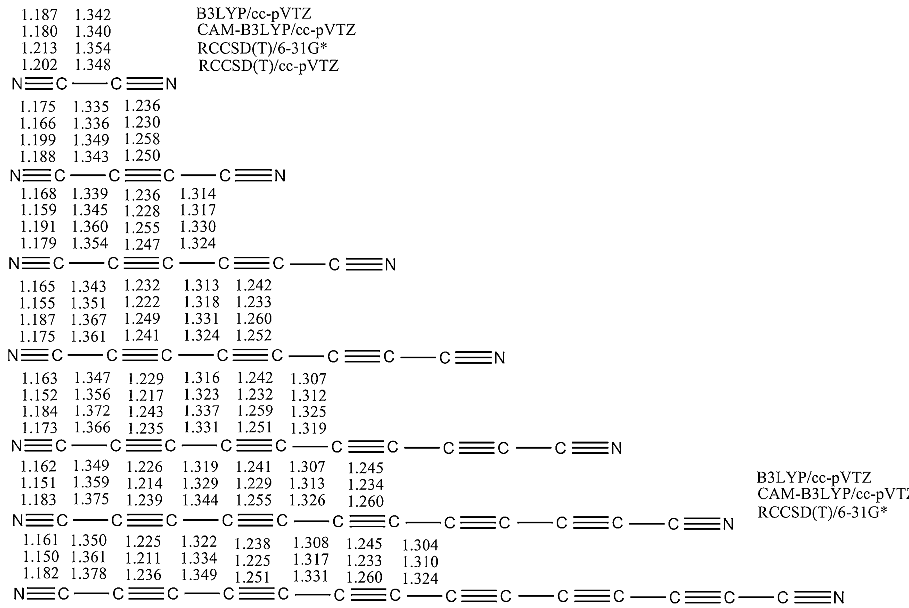

by B3LYP. In addition, the acetylenic bonding can disperse the positive charge in $NC_{2n}N^+$ through conjugation interaction, and it will stabilize the cationic clusters.

With regard to RCCSD(T) approach, the maximum deviation of the optimized bond lengths by cc-pVTZ basis set and the 6-31G* basis set is 0.012 Å, indicating that the RCCSD(T)/6-31G* is a cost-effective level of theory yielding the reliable results in the structural calculations of these species. Therefore, we employed RCCSD(T)/6-31G* to optimize the chains of $NC_{2n}N^+$ ($n = 1$–7) in the present work and implemented RCCSD(T)/cc-pVTZ to compute the chains of $NC_{2n}N^+$ ($n = 1$–5). Moreover, we find that at the RCCSD(T)/6-31G* level of theory, the carbon–carbon triple bond length is between 1.236 and 1.260 Å, and carbon–carbon single bond lengths are between 1.324 and 1.378 Å.

In order to further understand the BLA feature, we take the optimized equilibrium configurations of NC_8N^+ and NC_8N [9] as representative species for comparison in Fig. 2. As can be seen in Fig. 2, the BLA feature in NC_8N is slightly more remarkable than the corresponding NC_8N^+, and the differences between the single and triple bond lengths are in the range of 0.139–0.201 Å for NC_8N and 0.071–0.180 Å for NC_8N^+, respectively. Owing to loss of one electron, the π-bonding interaction in NC_8N^+ is less localized than that in NC_8N, and the extended conjugated interactions can stabilize the cation.

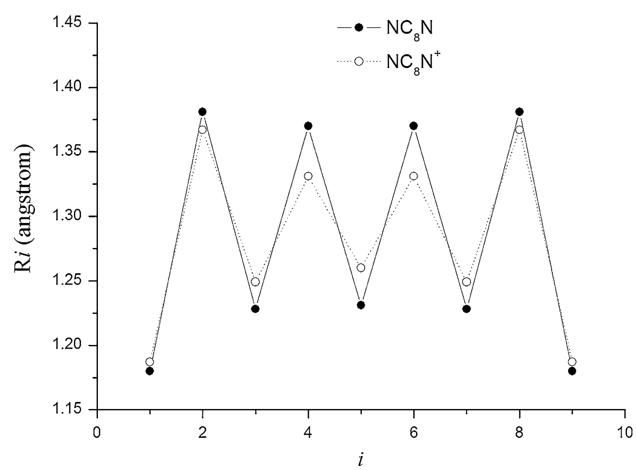

Fig. 2 Optimized of all bond lengths of NC_8N^+ and NC_8N [9] for the ground state at the RCCSD(T)/6-31G* level. "i" is numbered starting from one to the other

3.1.2 Rotational constants

Table 2 lists the calculated rotational constants (B_e) for $NC_{2n}N^+$ ($n = 1$–7) using the optimized geometries above. In previous study [20, 21], the RCCSD(T) approach is reliable for rotational constants calculations. Moreover, the calculated results by RCCSD(T) method with cc-pVTZ and 6-31G* basis sets are almost the same in this paper. Therefore, considering the computational cost, we carry out the curve fitting by RCCSD(T)/6-31G* for $NC_{2n}N^+$ ($n = 1$–7):

$$\log B_e(\text{MHz}) = A + Bn + Cn^2 + Dn^3 + En^4, \tag{2}$$

where $A = 4.4407$, $B = -0.9401$, $C = 0.1755$, $D = -0.0198$, and $E = 9.0956 \times 10^{-4}$. The fitting error and correlation coefficient are 9.1542×10^{-6} and 1, respectively, showing high accuracy. In addition, as the chain size increases, the calculated rotational constant gradually decreases from 4.5466 to 0.0702 GHz from NC_2N^+ to $NC_{14}N^+$. It is noticeable that for $NC_{2n}N^+$ ($n = 1$–3), our

Table 2 The calculated rotational constants (B_e in cm^{-1}) of $NC_{2n}N^+$ (n = 1–7)

	B_e				B_0
	RCCSD(T)/6-31G*	RCCSD(T)/cc-pVTZ	B3LYP/cc-pVTZ	CAM-B3LYP/cc-pVTZ	Expt.
NC_2N^+	4.5466	4.6171	4.7027	4.7402	4.6767 (24)[a]
NC_4N^+	1.3078	1.3252	1.3490	1.3563	1.3396 (72)[b]
NC_6N^+	0.5509	0.5576	0.5682	0.5705	0.5622 (05)[c]
NC_8N^+	0.2835	0.2868	0.2922	0.2932	
$NC_{10}N^+$	0.1649	0.1668	0.1700	0.1705	
$NC_{12}N^+$	0.1043		0.1075	0.1079	
$NC_{14}N^+$	0.0702		0.0724	0.0726	

[a] From Ref. [52]

[b] From Ref. [53]

[c] From Ref. [54]

calculations by Eq. 2 agree well with the available experimental data (B_0) [52–54] of 4.6767, 1.3395, and 0.5622 GHz, respectively, and the absolute errors between experimental values and the results by fitting curve are 0.135, 0.025, and 0.014 GHz. It can be seen that our fitting is reliable. Meanwhile, the calculations by B3LYP and CAM-B3LYP approach with cc-pVTZ basis set also provide the comparable rotational constants.

3.1.3 Stabilities

For the further insight into the nature of the optimized structures, we collect, in Table 3, the harmonic vibrational frequencies of $NC_{2n}N^+$ (n = 1–7) chain theoretical prediction at the B3LYP/cc-pVTZ level. We find that the lowest bending frequencies of $NC_{2n}N^+$ (n = 1–7) are 193, 102, 60, 40, 28, 21, and 16 cm^{-1}, respectively, all of which are real, suggesting that these cationic radicals are stable on the potential energy surface. Besides, very low vibrational frequencies suggest a shallow potential with respect to the corresponding normal coordinate, and the lowest bending frequencies are gradually decreasing accompany with the increasing of n. To understand the stability of these cationic species deeply, the dissociation has also been considered. The ground state of clusters $NC_{2n}N^+$ (n = 1–7) have BLA character, thus, carbon–carbon single bond is more easily broken, therefore, we mainly compute dissociated energies of them at B3LYP/cc-pVTZ level. The clusters lose –C≡C– group because of carbon–carbon single bond dissociation, which would need 496, 482, 475, 471, 468, 467 kcal mol^{-1} for $NC_{2n}N^+$ (n = 2–7), respectively. Therefore, we find that the chains is longer, the dissociated energies needed is lower, that means, the stability is poorer with the increasing of chains, which is consistent with our frequencies analyze. Moreover, we find that the clusters $NC_{2n}N^+$ lose –C≡C–C≡C–, –C≡C–C≡C–C≡C–, –C≡C–C≡C–C≡C–C≡C–, –C≡C–C≡C–C≡C–C≡C–C≡C– groups as the carbon–carbon single bond dissociation can obtain the same conclusion.

3.2 CASSCF optimized geometries of the $X^2\Pi_{g/u}$ and $1^2\Pi_{u/g}$ state

Figure 3 depicts the CASSCF optimized geometries with 6-31G* basis set of the $X^2\Pi_{g/u}$ ground state and $1^2\Pi_{u/g}$ excited state for the $NC_{2n}N^+$ (n = 1–7) carbon clusters. Considering the converged problem of the states, we select three π_u ($2\pi_u$–$4\pi_u$) and three π_g ($2\pi_g$–$4\pi_g$) orbitals for the active spaces of $NC_{12}N^+$, and for the other species, the active spaces are consistent with those in Table 1. As can be seen in Fig. 3, we find that the bond length of N–C generally decreases as the chain size increases for $NC_{2n}N^+$ (n = 2–7), and both of the $X^2\Pi_{g/u}$ ground state and $1^2\Pi_{u/g}$ excited state have the character of bond length alternation for $NC_{2n}N^+$ (n = 1–7), which has been long established according to Su–Schrieffer–Heeger's model for polyacetylene [38, 39] that the electronic excitations in conjugated chains should possess local character.

3.3 Vertical excitation energies

The cationic chains $NC_{2n}N^+$ (n = 1–7) are in $^2\Pi_{g/u}$ ground states arising from a π_g^3 or π_u^3 electronic configuration.

The charge always to be delocalized in DFT, while the RCCSD(T) approach can predict more reliable local deformation than the DFT approaches. In present work, local deformation plays an important role in the structure of ground states and excited states for linear clusters $NC_{2n}N^+$. Therefore, we calculate the electronic configuration, vertical excitation energies (ΔE), and oscillator strengths (f) of the dipole-allowed $(1, 2, 3)^2\Pi_{u/g} \leftarrow X^2\Pi_{g/u}$ transitions as well as the dipole-forbidden $1^2\Phi_{u/g} \leftarrow X^2\Pi_{g/u}$ transitions for the chains $NC_{2n}N^+$ by CASPT2 method with the cc-pVTZ basis set at the RCCSD(T)/6-31G* and RCCSD(T)/

Table 3 The calculated harmonic vibrational frequencies (in cm^{-1}) of $NC_{2n}N^+$ (n = 1–7) in their ground states by B3LYP/cc-pVTZ

Species	Mode	Vibrational frequencies
NC_2N^+	σ_g	909, 2,298
	σ_u	1,921
	π_g	430, 524
	π_u	**193**, 225
NC_4N^+	σ_g	631, 2,033, 2,303
	σ_u	1,236, 2,126
	π_g	252, 261, 529, 567
	π_u	**102**, 109, 434, 486
NC_6N^+	σ_g	485, 1,392, 2,179, 2,254
	σ_u	942, 2,056, 2,186
	π_g	160, 164, 423, 460, 528, 580
	π_u	**60**, 63, 280, 283, 511, 533
NC_8N^+	σ_g	394, 1,128, 2,055, 2,184, 2,246
	σ_u	768, 1,478, 2,161, 2,206
	π_g	107, 109, 292, 301, 493, 511, 529, 582
	π_u	**40**, 41, 202, 202, 413, 442, 521, 554
$NC_{10}N^+$	σ_g	332, 957, 1,532, 2,127, 2,164, 2,265
	σ_u	650, 1,249, 2,049, 2,148, 2,250
	π_g	75, 77, 227, 230, 405, 429, 508, 531, 536, 580
	π_u	**28**, 29, 145, 146, 301, 312, 478, 484, 527, 563
$NC_{12}N^+$	σ_g	287, 831, 1,332, 2,041, 2,073, 2,205, 2,273
	σ_u	562, 1,089, 1,568, 2,113, 2,152, 2,277
	π_g	56, 58, 175, 175, 307, 319, 466, 480, 516, 533, 548, 579
	π_u	**21**, 21, 109, 110, 246, 251, 399, 420, 497, 520, 531, 566
$NC_{14}N^+$	σ_g	252, 735, 1,186, 1,592, 2,024, 2,137, 2,208, 2,285
	σ_u	496, 966, 1,392, 2,034, 2,075, 2,199, 2,289
	π_g	44, 45, 137, 138, 260, 266, 394, 413, 487, 507, 520, 536, 554, 577
	π_u	**16**, 17, 84, 86, 197, 198, 312, 324, 455, 468, 508, 534, 534, 567

Bold values indicate the lowest bending frequencies for clusters $NC_{2n}N^+$ (n = 1–7)

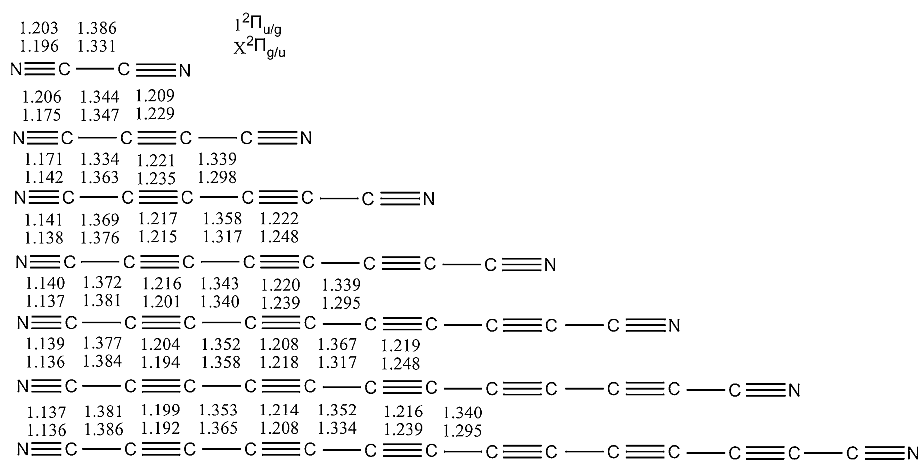

Fig. 3 CASSCF–optimized geometries (in Å) of $X^2\Pi_{g/u}$ and $1^2\Pi_{u/g}$ for $NC_{2n}N^+$ (n = 1–7) cations

cc-pVTZ equilibrium geometry, respectively. Table 4 summarizes our calculated results referred above and the available experimental data along with the previous theoretical data which calculated at CASPT2/D2VP level with UHF/4-31G optimized structures. Fig. 4 displays the relative energy levels of the selected excited states in $NC_{2n}N^+$ (n = 1–7). It is interesting to find that the maximum deviation from experimental results is 0.04 eV between the gas phase [10] and the 5 K neon matrixes [10–12]. In addition, compared with these experimental values, our calculations using the RCCSD(T)/6-31G* optimized geometries can give comparable results.

Table 4 The calculated vertical excitation energies (ΔE in eV) and oscillator strengths (f) for $NC_{2n}N^+$ (n = 1–8) by CASPT2 method

Species	State	Transition	CASPT2//RCCSD(T)			
			ΔE^a	f^a	ΔE^b	f^b
NC_2N^+	$X^2\Pi_g$	$\ldots 1\pi_u^4 4\sigma_u^2 5\sigma_g^2 1\pi_g^3$	0.00		0.00	
	$1^2\Pi_u$	$1\pi_u \rightarrow 1\pi_g$	2.26 (2.11)[c] {2.15}[d]	3.36×10^{-2}	2.30	3.52×10^{-2}
	$2^2\Pi_u$	$1\pi_g \rightarrow 2\pi_u$	4.35 {4.16}[d]	1.99×10^{-2}	4.48	1.95×10^{-2}
	$1^2\Phi_u$	$1\pi_g \rightarrow 2\pi_u$	5.02	0	5.15	0
	$3^2\Pi_u$	$1\pi_g \rightarrow 2\pi_u$	5.62	1.88×10^{-2}	5.75	1.83×10^{-2}
NC_4N^+	$X^2\Pi_u$	$\ldots 6\sigma_u^2 7\sigma_g^2 1\pi_g^4 2\pi_u^3$	0.00		0.00	
	$1^2\Pi_g$	$1\pi_g \rightarrow 2\pi_u$	2.09 (2.07)[e] {2.08}[d] [2.09][f]	2.74×10^{-2}	2.14	2.94×10^{-2}
	$2^2\Pi_g$	$2\pi_u \rightarrow 2\pi_g$	3.29 {3.16}[d]	8.51×10^{-3}	3.38	8.44×10^{-3}
	$1^2\Phi_g$	$2\pi_u \rightarrow 2\pi_g$	3.82	0	3.90	0
	$3^2\Pi_g$	$2\pi_u \rightarrow 2\pi_g$	4.30	6.28×10^{-3}	4.39	6.20×10^{-3}
NC_6N^+	$X^2\Pi_g$	$\ldots 8\sigma_u^2 9\sigma_g^2 2\pi_u^4 2\pi_g^3$	0.00		0.00	
	$1^2\Pi_u$	$2\pi_u \rightarrow 2\pi_g$	1.91 (1.88)[e] {1.89}[d] [1.85][f]	9.92×10^{-2}	1.94	1.02×10^{-1}
	$2^2\Pi_u$	$2\pi_g \rightarrow 3\pi_u$	2.42	1.56×10^{-2}	2.49	1.72×10^{-2}
	$1^2\Phi_u$	$2\pi_g \rightarrow 3\pi_u$	2.76	0	2.84	0
	$3^2\Pi_u$	$2\pi_g \rightarrow 3\pi_u$	3.26 {3.17}[d]	1.66×10^{-2}	3.33	1.99×10^{-2}
NC_8N^+	$X^2\Pi_u$	$\ldots 10\sigma_u^2 11\sigma_g^2 2\pi_g^4 3\pi_u^3$	0.00		0.00	
	$1^2\Pi_g$	$2\pi_g \rightarrow 3\pi_u$	1.72 (1.67)[d] [1.57][f]	8.09×10^{-2}	1.75	8.17×10^{-2}
	$2^2\Pi_g$	$3\pi_u \rightarrow 3\pi_g$	2.21	1.44×10^{-2}	2.27	1.41×10^{-2}
	$1^2\Phi_g$	$3\pi_u \rightarrow 3\pi_g$	2.54	0	2.60	0
	$3^2\Pi_g$	$3\pi_u \rightarrow 3\pi_g$	2.96	1.28×10^{-2}	3.02	1.25×10^{-2}
$NC_{10}N^+$	$X^2\Pi_g$	$\ldots 12\sigma_u^2 13\sigma_g^2 2\pi_g^4 3\pi_u^4 3\pi_g^3$	0.00		0.00	
	$1^2\Pi_u$	$3\pi_u \rightarrow 3\pi_g$	1.56 (1.49)[d] [1.70][f]	1.45×10^{-1}	1.59	1.46×10^{-1}
	$2^2\Pi_u$	$3\pi_g \rightarrow 4\pi_u$	1.95	1.93×10^{-2}	2.00	1.90×10^{-2}
	$1^2\Phi_u$	$3\pi_g \rightarrow 4\pi_u$	2.24	0	2.28	0
	$3^2\Pi_u$	$3\pi_g \rightarrow 4\pi_u$	2.62	1.63×10^{-2}	2.67	1.62×10^{-2}
$NC_{12}N^+$	$X^2\Pi_u$	$\ldots 14\sigma_u^2 15\sigma_g^2 3\pi_u^4 3\pi_g^4 4\pi_u^3$	0.00			
	$1^2\Pi_g$	$3\pi_g \rightarrow 4\pi_u$	1.39 (1.34)[d] [1.34][f]	1.88×10^{-1}		
	$2^2\Pi_g$	$4\pi_u \rightarrow 4\pi_g$	1.82	2.52×10^{-2}		
	$1^2\Phi_g$	$4\pi_u \rightarrow 4\pi_g$	2.08	0		
	$3^2\Pi_g$	$4\pi_u \rightarrow 4\pi_g$	2.43	2.43×10^{-2}		
$NC_{14}N^+$	$X^2\Pi_g$	$\ldots 16\sigma_u^2 17\sigma_g^2 3\pi_u^4 3\pi_g^4 4\pi_u^4 4\pi_g^3$	0.00			
	$1^2\Pi_u$	$4\pi_u \rightarrow 4\pi_g$	1.20	2.41×10^{-1}		
	$2^2\Pi_u$	$4\pi_g \rightarrow 5\pi_u$	1.38	1.34×10^{-2}		
	$1^2\Phi_u$	$4\pi_g \rightarrow 5\pi_u$	1.56	0		
	$3^2\Pi_u$	$4\pi_g \rightarrow 5\pi_u$	1.96	1.21×10^{-2}		

The values in parentheses, braces are the experimental data obtained in 5 K neon matrixes and gas phase, and the values in square brackets are previous theoretical data calculated at CASPT2/D2VP//UHF/4-31G level

[a] CASPT2/cc-pVTZ//RCCSD(T)/6-31G*

[b] CASPT2/cc-pVTZ//RCCSD(T)/cc-pVTZ

[c] From Ref. [11]

[d] From Ref. [10]

[e] From Ref. [12]

[f] From Ref. [13]

The lowest excited state is found to be $1^2\Pi_{u/g}$ among the selected four excited electronic states, derived from the next highest occupied molecular orbital (HOMO-1) to the highest occupied molecular orbital (HOMO) orbital ($\pi \rightarrow \pi$) for NC_2N^+, and HOMO-3 orbital to HOMO orbital ($\pi \rightarrow \pi$) for $NC_{2n}N^+$ (n = 2–7). The calculated vertical excitation energies from $1^2\Pi_{u/g} \leftarrow X^2\Pi_{g/u}$ of $NC_{2n}N^+$ (n = 1–6) are 2.26, 2.09, 1.91, 1.72, 1.56, and

1.39 eV, respectively, in a good accord with the available experimental values of 2.11, 2.07, 1.88, 1.67, 1.49, and 1.34 eV obtained in the 5 K neon matrixes by Maier et al. [10–12]. Our calculated results are much better than the previous theoretical data for most species [13, 17]. Therefore, we calculate the vertical excitation energy of $1^2\Pi_{u/g} \leftarrow X^2\Pi_{g/u}$ for the longer chain $NC_{14}N^+$ at the same level, and the value obtained is 1.20 eV. We hope that the present theoretical study is useful and reasonable in future experiment study on the molecule. In addition, we also obtain the oscillator strengths from $1^2\Pi_{u/g} \leftarrow X^2\Pi_{g/u}$ for the chains $NC_{2n}N^+$ ($n = 1$–7). The corresponding oscillator strengths are 3.36×10^{-2}, 2.74×10^{-2}, 9.92×10^{-2}, 8.09×10^{-2}, 1.45×10^{-1}, 1.88×10^{-1}, and 2.41×10^{-1}, respectively, thus, we can see clearly that the electronic spectra become more accessible to the longer carbon chains experimentally.

As Table 4 and Fig. 4 display, the relative energy level of selected three low-lying excited states ($2^2\Pi_{u/g}$, $1^2\Phi_{u/g}$, and $3^2\Pi_{u/g}$) in $NC_{2n}N^+$ ($n = 1$–7) has a similar fashion. The electron promotions from the ground state to the $2^2\Pi_{u/g}$, $1^2\Phi_{u/g}$, and $3^2\Pi_{u/g}$ excited states are ascribed to the excitation from the HOMO to the lowest unoccupied molecular orbital (LUMO). As Table 4 lists, the vertical excitation energies of $2^2\Pi_{g/u}$ state of $NC_{2n}N^+$ ($n = 1$–7) were computed as 4.35, 3.29, 2.42, 2.21, 1.95, 1.82, and 1.38 eV above the ground state energy, respectively. The experimental data obtained in the gas phase are 4.16 and 3.16 eV for $NC_{2n}N^+$ ($n = 1$–2), thus, we can see that our calculations are close to the available experimental values with maximum deviation of 0.19 eV [10]. The corresponding oscillator strengths are 1.99×10^{-2}, 8.51×10^{-3}, 1.56×10^{-2}, 1.44×10^{-2}, 1.93×10^{-2}, 2.52×10^{-2}, and 1.34×10^{-2}, therefore, $2^2\Pi_{u/g} \leftarrow X^2\Pi_{g/u}$ transitions can be detectable in the experiments. The $1^2\Phi_{u/g}$ states are 5.02, 3.82, 2.76, 2.54, 2.24, 2.08, and 1.56 eV above the ground state, respectively. The calculated vertical excitation energies of $3^2\Pi_{u/g} \leftarrow X^2\Pi_{g/u}$ are 5.62, 4.30, 3.26, 2.96, 2.62, 2.43, and 1.96 eV, respectively. The relatively strong transition of NC_6N^+ at 3.26 eV should be responsible for the experimental band at 3.17 eV [10]. Their corresponding f values are 1.88×10^{-2}, 6.28×10^{-3}, 1.66×10^{-2}, 1.28×10^{-2}, 1.63×10^{-2}, 2.43×10^{-2}, and 1.21×10^{-2}, respectively, so the $3^2\Pi_{u/g} \leftarrow X^2\Pi_{g/u}$ transitions can also be observed in further experiment. Because of the agreement of our calculations and experimental values, we believe that this approach is reliable on this system and could provide useful information for the further experiment.

3.4 Size dependence of vertical excitation energies

Experimentally, Maier et al. indicated that the absorption wavelengths of bands origin (λ in nm) obtained of $NC_{2n}N^+$ ($n = 1$–6) chains for the $1^2\Pi_{u/g} \leftarrow X^2\Pi_{g/u}$ transitions show the prominently nonlinear size dependence. Therefore, the nonlinear size dependence along with the corresponding calculated results for $NC_{2n}N^+$ ($n = 1$–7) by CASPT2 theory with cc-pVTZ basis set at the RCCSD(T)/6-31G* equilibrium geometry can be seen in Fig. 5. The nonlinear fitting yields the following equation:

$$\lambda = A \exp(n/B) + C, \qquad (3)$$

where n is half of the total carbon atoms, and the expression (λ[nm] = 1,239.824 [nm × eV]/ΔE [eV]) is used. Moreover, in order to compare with the experimental data and our calculations, the previous theoretical values cal-

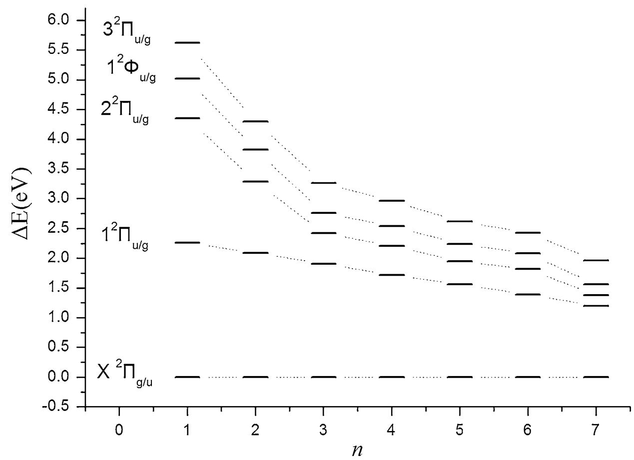

Fig. 4 Relative energy levels of the four electronic states in $NC_{2n}N^+$ ($n = 1$–7)

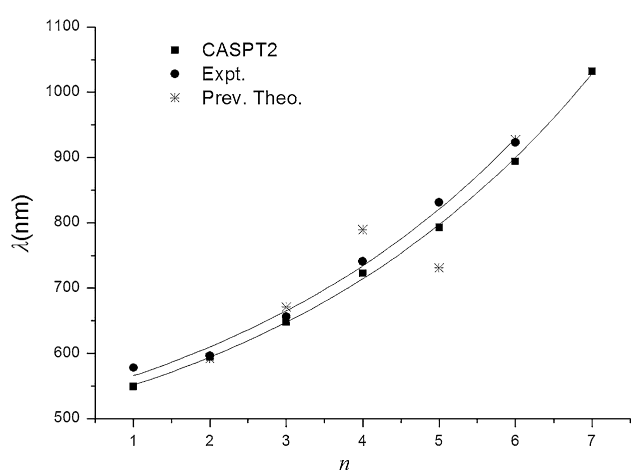

Fig. 5 The nonlinear size dependence of the *vertical* excitation energies of the $1^2\Pi_{u/g} \leftarrow X^2\Pi_{g/u}$ transitions for $NC_{2n}N^+$ ($n = 1$–7) cations at the CASPT2/cc-pVTZ//RCCSD(T)/6-31G* level along with the experimental values [10–12] and previous theoretical data at CASPT2/D2VP//UHF/4-31G level [13]

culated at CASPT2/D2VP//UHF/4-31G level are also draw in Fig. 5.

As Fig. 5 shows, in the case of experimental values, $A = 139.62$, $B = 4.45$, and $C = 391.01$. The correlation coefficient is 0.99821, indicating high accuracy. For the theoretical equation, $A = 141.68$, $B = 4.58$, and $C = 374.89$. The correlation coefficient is 0.99916, with a good reproducibility. Moreover, we note that both fitting curves match very well. Meanwhile, the previous calculations display poor nonlinear dependence.

In order to carry out a much deeper research on the size dependence of vertical excitation energies for $NC_{2n}N^+$ ($n = 1$–7), previous studies on the neutral $NC_{2n}N$ [8, 9] were brought to make a comparison. Scemama et al. [8] and Zhang et al. [9] obtained the same vertical excitation energies with ZINDO [55] and TD–DFT approaches, respectively, and the absorption wavelengths of the bands origin for the $^1\Sigma_u^+ \leftarrow X^1\Sigma_g^+$ transitions of $NC_{2n}N$ were found to have the nonlinear size dependence $\lambda = 1{,}240.6 \times (1.35961–1.15577/1.05908^n)/[2 + (3n + 6)^{1/2}–(3n + 3)^{1/2}]$ [9]. The two nonlinear size dependences are different, which may be caused by the character of their geometries in the excited state with respect to the ground state.

4 Conclusions

In this work, we report the equilibrium configuration and electronic spectra for the cationic chains $NC_{2n}N^+$ ($n = 1$–7). The $NC_{2n}N^+$ clusters are observed to have the character of bond length alternation (BLA) in both the $X^2\Pi_{g/u}$ ground state and $1^2\Pi_{u/g}$ excited state. The oscillator strengths of the $1^2\Pi_{u/g} \leftarrow X^2\Pi_{g/u}$ transitions for the longer chains are bigger than the shorter chains. Therefore, the electronic spectra become more detectable for the longer carbon chains in experiment. Moreover, for the dipole-allowed $(1, 2, 3)^2\Pi_{u/g} \leftarrow X^2\Pi_{g/u}$ transitions, our calculations by CASPT2 method are consistent with the available experimental values. In addition, the absorption wavelengths of bands for the $1^2\Pi_{u/g} \leftarrow X^2\Pi_{g/u}$ transitions exhibit significant nonlinear size dependence. Overall, the present calculations provide accurate information for spectroscopists, and they offer a basis for understanding of the excited state properties of these cyanopolyacetylene cations, thus, they should be helpful to further experimental and theoretical work.

Acknowledgments The authors thank the State Key Laboratory of Physical Chemistry of Solid Surfaces for providing computational resources and the National Science Foundation of China (Grant No. 21003036) and Science Foundation of Henan University (Grant No. SBGJ090507) for financial supports.

References

1. Kroto HW (1981) Int Rev Phys Chem 1:309
2. Thaddeus P, Gottlieb CA, Mollaaghababa R, Vrtilek JM (1993) J Chem Soc Faraday Trans 89:2125
3. Bell MB, Feldman PA, Kwok S, Matthews HE (1982) Nature 295:389
4. Kroto HW (1978) New Sci 83:400
5. Howe DA, Miller TJ (1990) Mon Not R Astron Soc 244:444
6. Jochnowitz EB, Maier JP (2008) Annu Rev Phys Chem 59:519
7. Scemama A, Chaquin P, Gazeau MC, Bénilan Y (2002) J Phys Chem A 106:3828
8. Scemama A, Chaquin P, Gazeau MC, Bénilan Y (2002) Chem Phys Lett 361:520
9. Zhang JL, Wu WP, Wang LB, Cao ZX (2005) Chinese J Struct Chem 24:885
10. Nagarajan R, Maier JP (2010) Int Rev Phys Chem 29:521
11. Fulara J, Leutwyler S, Maier JP, Spittel U (1985) J Phys Chem 89:3190
12. Forney D, Freivogel P, Fulara J, Maier JP (1995) J Chem Phys 102:22
13. Lee JM, Adamowicz L (2001) Spectrochim Acta Part A 57:897
14. Andersson K, Malmqvist P-A, Roos BO, Sadlej AJ, Wolinski K (1990) J Phys Chem 94:5483
15. Andersson K, Malmqvist P-A, Roos BO (1992) J Chem Phys 96:1218
16. Andersson K, Roos BO (1994) In: Yarkony R (ed) Modern electron structure theory. World scientific, New York, p 1
17. Cao ZX, Peyerimhoff SD (2001) J Phys Chem A 105:627
18. Celani P, Werner H-J (2000) J Chem Phys 112:5546
19. Zhang JL, Wu WP, Wang LB, Chen X, Cao ZX (2006) J Phys Chem A 110:10324
20. Zhang JL, Guo XG, Cao ZX (2009) J Chem Phys 131:144307
21. Zhang JL, Guo XG, Cao ZX (2010) Int J Mass Spectrom 290:113
22. Watts JD, Gauss J, Bartlett RJ (1993) J Chem Phys 98:8718
23. Knowles PJ, Hampel C, Werner H-J (1993) J Chem Phys 99:5219
24. Knowles PJ (2000) J Chem Phys 112:3106
25. Woon DE, Dunning TH Jr (1993) J Chem Phys 98:1358
26. Kendall RA, Dunning TH Jr, Harrison RJ (1992) J Chem Phys 96:6796
27. Dunning TH Jr (1989) J Chem Phys 90:1007
28. Peterson KA, Woon DE, Dunning TH Jr (1994) J Chem Phys 100:7410
29. Wilson A, Mourik T, Dunning TH Jr (1997) J Mol Struct (Theochem) 388:339
30. Ditchfield R, Hehre WJ, Pople JA (1971) J Chem Phys 54:724
31. Hehre WJ, Ditchfield R, Pople JA (1972) J Chem Phys 56:2257
32. Hariharan PC, Pople JA (1974) Mol Phys 27:209
33. Gordon MS (1980) Chem Phys Lett 76:163
34. Hariharan PC, Pople JA (1973) Theo Chim Acta 28:213
35. Blaudeau J-P, McGrath MP, Curtiss LA, Radom L (1997) J Chem Phys 107:5016
36. Francl MM, Pietro WJ, Hehre WJ, Binkley JS, DeFrees DJ, Pople JA, Gordon MS (1982) J Chem Phys 77:3654
37. Binning RC Jr, Curtiss LA (1990) J Comp Chem 11:1206
38. Rassolov VA, Pople JA, Ratner MA, Windus TL (1998) J Chem Phys 109:1223
39. Rassolov VA, Ratner MA, Pople JA, Redfern PC, Curtiss LA (2001) J Comp Chem 22:976
40. Clark T, Chandrasekhar J, Spitznagel GW, Schleyer PR (1983) J Comp Chem 4:294
41. Lee C, Yang W, Parr RG (1988) Phys Rev B 37:785
42. Miehlich B, Savin A, Stoll H, Preuss H (1989) Chem Phys Lett 157:200
43. Becke AD (1993) J Chem Phys 98:5648

44. Yanai T, Tew DP, Handy NC (2004) Chem Phys Lett 393:51
45. Werner H-J, Knowles PJ (1985) J Chem Phys 82:5053
46. Knowles PJ, Werner H-J (1985) Chem Phys Lett 115:259
47. Wilson A, Mourik T, Dunning TH Jr (1997) J Mol Struct (Theochem) 388:339
48. Peyerimhoff SD (1998) In: Schleyer PVR, Allinger NL, Clark T, Gasteiger J, Kollman PA, Schaefer HF, Schreiner PR (eds) The encyclopedia of computational chemistry, vol 4. Wiley, New York, p 2654
49. Frisch MJ, Trucks GW, Schlegel HB et al (2009) GAUSSIAN09. Revision A.02. Gaussian Inc, Wallingford CT
50. MOLPRO, A package of ab initio programs, Werner H-J, Knowles PJ (2006) (see http://www.molpro.net for more details)
51. Peach MJG, Tellgren EI, Salek P, Helgaker T, Tozer DJ (2007) J Phys Chem A 111:11930
52. Rudnev V, Rice CA, Maier JP (2008) J Chem Phys 129:134315
53. Sinclair WE, Pfluger D, Maier JP (1999) J Chem Phys 111:9600
54. Linnartz H, Pfluger D, Vaizert O, Cias P, Birza P, Khoroshev D, Maier JP (2002) J Chem Phys 116:924
55. Zerner MC, Ridley JE (1973) Theor Chim Acta (Berlin) 32:111